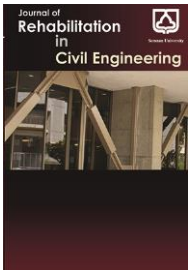

journal homepage: http://civiljournal.semnan.ac.ir/

Response of Buildings with Inclined First-Story Columns to Near-Fault Ground Motion

F. Rouzmehr[1] and R. Saleh Jalali[2*]

1.MS student, Department of Civil Engineering, Faculty of Engineering, University of Guilan, PO Box 3756, Rasht, Iran.
2.Assistant Professor, Department of Civil Engineering, Faculty of Engineering, University of Guilan, PO Box 3756, Rasht, Iran.

Corresponding author: *saleh@guilan.ac.ir*

ARTICLE INFO

Article history:
Received: 20 August 2014
Accepted: 22 October 2014

Keywords:
Near-fault earthquake,
Forward directivity pulse,
Inclined first-story column,
Nonlinear response.

ABSTRACT

In this paper a simple model of a three story building with inclined first-story columns has presented. The stories are supposed to be rigid and are connected to axially rigid mass less columns by elasto-plastic rotational springs and linear rotational dampers. The considered model is subjected to horizontal component of fault normal pulse with different magnitudes and the governed nonlinear differential equations of motion have been solved by the forth order Runge-Kutta method. Results indicate that the inclination of the first-story columns stiffens the system. However, the change of the frequency of the first mode is small. The deformation of the first story with inclined columns is such that it forces the building in a pendulum-like motion. So it would be possible to reduce the relative building response. Results indicate that an optimum value of inclination angle of the first-story columns is $\alpha = 10^{\circ}$. Under this condition the first-story drift decreases while upper-story drift increases, respect to the common building with $\alpha = 0$. For larger inclination angles the gravity effect leads to increase the first-story drift as well. This solution would be useful in earthquake resistant design of buildings with architectural limitations at the first story.

1. Introduction

In the near field of strong earthquakes, and especially close to surface faults, the strong ground motion can be dominated by the permanent displacements (typically parallel to the fault surface) and by large pulses (often perpendicular to the fault). Traces of

these large displacements and pulses are not always obvious in the processed records of the recorded motions because of the band-pass filtering [1-3].

It is customary in the analyses of the response of structures to strong earthquake ground motion to neglect the effects of the propagating character of the wave motion in the ground. In those studies it is assumed that the seismic waves arrive simultaneously at various points of the base of the structure. This corresponds either to vertical wave incidence (i.e. to infinite phase velocity along the ground surface), or to waves with angle of incidence other than zero, but with very large wavelengths compared to the size of the base of the structure. However, in general, the seismic waves arrive towards the foundation with incident angles other than vertical, and may have wavelengths comparable with the horizontal dimensions of the structure, resulting in phased excitation at its base. When the distances between the multiple support points are large (bridges, dams, tunnels, long buildings), the effects of differential motions become important and should be considered in dynamic analyses [4]. Spatial and temporal stochastic representations of strong earthquake motion required for such analyses have been investigated in many papers and in a recent book by Zerva [5]. The consequences of differential ground motion have been studied for the bridges [6-8], long building [9-12], and dams [13-15]. However, with few exceptions, engineering applications of the response spectrum method ignore the wave propagation effects in the foundation soil, or consider only a simplified stochastic representation of the differences in motion among separate supports. Okubo et al [16] were among the first to measure and interpret finite ground strains of recorded earthquake motions, for plan dimensions representative of intermediate and large buildings. They showed that for short-period (stiff) structures, finite ground strains lead to increased base shears. Zembaty and Krenk [17, 18] studied the same problem and addressed explicitly the contribution of quasi-static and dynamic terms to the response. They showed that although the relative response of the structure is reduced in case of differential motion of supports (due to ‘averaging’ of spatially correlated motions), the shear forces in the columns, maybe significantly larger than for synchronous excitation. Jalali et al [19] showed that the combined action of horizontal, vertical, and rocking components of strong ground motion, near causative faults, combined with asynchronous excitation leads to drift amplitudes that are very large compared with the typical design drift amplitudes. An idea of passive base isolation of buildings using inclined soft first-story columns was explored by Todorovska [20]. She modeled the building by an equivalent SDOF oscillator and by neglecting of issues such as gravity, geometric nonlinearities, inelastic response, dynamic buckling of the inclined columns, and dynamic instability of the model for coupled horizontal and vertical responses in the near-field of strong earthquakes, indicated that due to inclination, in addition to stabilizing the system, it would also be possible to reduce the relative building response. She has also shown that for earthquake excitation the optimum inclination and its effectiveness will depend on the frequency content of the excitation and for broad band excitation an optimum value of the inclination angle is such that $0.05 < \frac{H}{h_R} < 0.1$. The purpose of the present study is to investigate the effect of

inclination angle of the first-story columns on maximum story drift of a simple three-storey building, by considering gravity, geometric nonlinearities, inelastic response, and dynamic instability of the model, subjected to horizontal component of near-source strong ground motion.

2. Dynamic model and solution of nonlinear equation of motion

The system of nonlinear equations of motion of the model in Fig. 1, which is described in the Appendix [by equation (A.7)] can be solved by numerical methods. We chose the fourth-order Runge-Kutta method because of its self-starting feature and the long-range stability. In this method, the time domain is divided into *n* equally spaced intervals, where *n* is chosen based on the requirement to have at least 20 points per period of excitation or per fundamental period of the structure, whichever is smaller. Each of these equally spaced intervals is further subdivided into 2^r intervals, where *r* varies from 1 to 9, to reach the desired accuracy. The parameter *r* is chosen so that the relative percent of error between the solutions for the neighboring two values of *n* is less than one percent, and then the larger *n* of the two is adopted for the calculations.

3. Near-fault ground motion

Strong ground motion near faults can be complicated due to irregular distribution of fault slip [1,3,21] because of non-uniform distribution of geologic rigidities surrounding the fault, non-uniform distribution of stress on the fault, and complex nonlinear processes that accompany faulting. Thus, in general it is not possible to predict the detailed nature of the near-fault ground motion and of the associated pulses. In this study, we adopt a simplified approach and model this motion by smooth pulse, which has correct average amplitude and duration, and which has been compared with and calibrated against the recorded strong motions in terms of their peak amplitudes in time and their spectral content.

Figure 2 shows schematically a fault and characteristic motion, d_F , which describe a pulse, with particle motion usually perpendicular to the fault and associated with failure of a nearby asperity or passage of dislocation under or past the observation point [22,23].

For the fault-normal pulse, we chose a pulse (Fig. 2):

$$d_F(t) = A_F t e^{-\alpha_F t} \tag{1}$$

Where the values of A_F , and α_F , for different earthquake magnitudes, are shown in Table 1 [24].

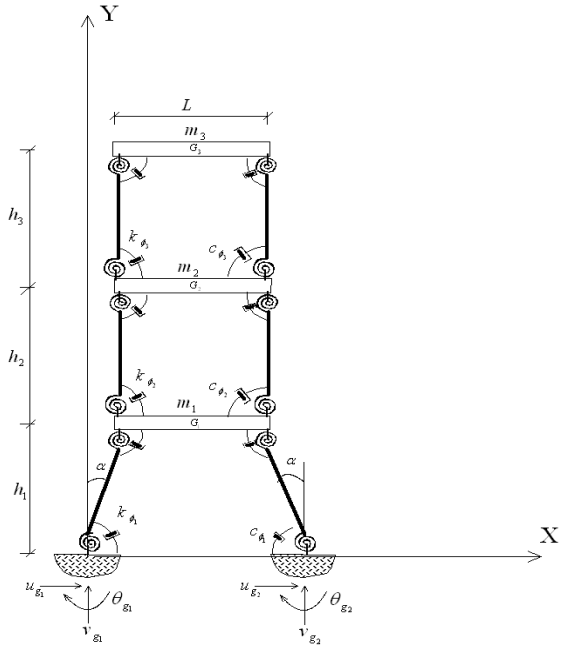

Fig.1. Model of a three-story building with inclined first-story columns subjected to differential horizontal, vertical, and rocking components of ground motions

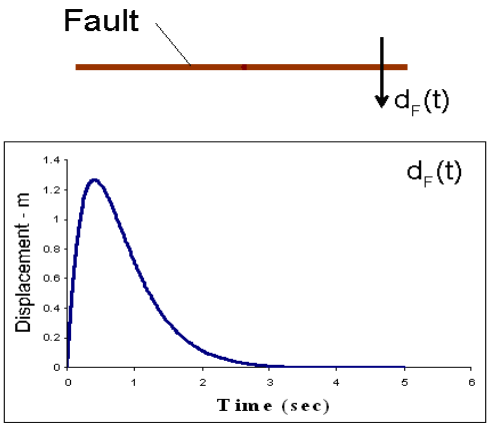

Fig. 2. Fault -normal (pulse), $d_F(t)$, ground displacement

Because the strong motion data are abundant only up to about M = 6.5, we place the values of α_F and A_F for M = 7 in Table 1 in parentheses to emphasize that those are based on extrapolation. The amplitude of has been studied in numerous regression analyses of recorded peak displacements at various distances from the fault.

An important physical property of d_F function, as used in this study, is its initial velocity. It can be shown that $\dot{d}_F \sim \sigma\beta/\mu$, where σ is the effective stress (~ stress drop) on the fault surface [23-25], β is the velocity of shear waves in the fault zone, and μ is the rigidity of rocks surrounding the fault. The largest peak velocity observed so far, 5 to 10 km above the fault, is about 200 cm/s. For example, 170 cm/s was recorded during the Northridge, California earthquake of 1994 [26]. Because there are no strong-motion measurements of peak ground velocity at the fault surface, the peak velocities $\dot{d}_F$ can be evaluated only indirectly in terms of σ. The accuracy of the stress estimates depends upon the assumptions and the methods used in interpretation of recorded strong-motion records, and it is typically about one order of magnitude. Therefore, solving the above equations for σ we can use $\sigma \sim \mu\dot{d}_F/\beta$ to check their consistency with other published estimates of σ [27].

Table1. Characteristics of the Fault-normal Pulse [24]

M (magnitude)	α_F (1/s)	A_F (cm /s)	$d_{F,\max}(cm)$	$\dot{d}_{F,\max}(cm/s)$
4	14.04	56.48	1.48	56.48
5	7.90	151.61	7.06	151.61
6	4.44	546.97	45.32	546.97
7	(2.50)	(860.34)	(126.6)	(860.34)

4. Structural response

The nature of relative motion of individual column foundations or of the entire foundation system will depend on the type of foundation and stiffness of the connecting beams and slabs, the characteristics of the soil surrounding the foundation, the type of incident waves, and the direction of wave arrival. In reality, at the base of each column, the motion has six degrees of freedom, which will depend on the foundation-soil interaction and on the degree to which the nonlinear deformations occur in

the structure and in the soil. In this paper, we consider simultaneous action of horizontal, vertical, and rocking components of ground motion, but we neglect the effects of foundation-soil interaction, and we perform the analysis for structures on separate foundations only. We assume that the structure is near the fault and that the longitudinal axis of the structure (X-axis) coincides with the radial direction (r-axis) of the propagation of waves from the earthquake source so that the absolute displacements of the bases of columns are different, because of the wave passage. However, we assume that the ground motion can be described approximately by linear wave motion. Thus, the nonlinear soil strains and cracks in the soil, which accompany violent strong ground motion, will not be considered. By considering the wave propagation from left to right in Fig. 1, we assume that the excitations at two piers have the same amplitude, but different phase. The phase difference (or time delay) between the two ground motions depends on the distance between piers and the horizontal phase velocity of the incident waves. As is seen from Fig. 1, the system is excited by differential horizontal, vertical, and rocking ground motions, $u_{g_i}, v_{g_i}, \theta_{g_i}, i = 1,2$, at the two bases. In this paper the building is subjected to synchronous horizontal ground motion so that

$$\begin{aligned} u_{g_2}(t) &= u_{g_1}(t) \\ v_{g_2}(t) &= v_{g_1}(t) = 0 \\ \theta_{g_2}(t) &= \theta_{g_1}(t) = 0 \end{aligned} \tag{2}$$

For illustrations in this work, it is assumed that L = 20 m and the height of each story is h1 = h2 = h3 =3.5 m. The first natural period of the system is supposed to be T1 = 0.3, and 0.6 sec. The damping ratio of the first mode is taken to be $\xi_1 = 0.02$. The material is assumed to be elasto-plastic, and the yielding limit of rotational springs of three stories is supposed to be ϕ_y = 0.01.

5. Results and discussion

In this paper, because of the inclined first-story columns and the differential motions of the ground at two piers, the relative rotation of each column at the top and at the bottom corners of each story will be different, and therefore the story drift is defined as follows:

$$Drift = \frac{\max\left\{h_1 \sin\left(\psi_{11} + \theta_{g_1} - \theta_{G_1}\right),\ h_1 \sin\left(\psi_{12} + \theta_{g_2} - \theta_{G_1}\right),\ h_1 \sin\left(\psi_{11}\right),\ h_1 \sin\left(\psi_{12}\right)\right\}}{h_1} \text{ (For the first story)}$$

$$Drift = \frac{\max\left\{h_i \sin\left(\phi_{i1} + \theta_{G_{i-1}} - \theta_{G_i}\right),\ h_i \sin\left(\phi_{i2} + \theta_{G_{i-1}} - \theta_{G_i}\right),\ h_i \sin\left(\phi_{i1}\right),\ h_i \sin\left(\phi_{i2}\right)\right\}}{h_i} \text{ (For } i\text{-}th \text{ story)} \tag{3}$$

Results indicate that the inclination of the first-story columns stiffens the system. However, the change of the frequency of the first mode is small. The deformation of the first story with inclined columns is such that it forces the building in a pendulum-like motion. Due to the inclination, in addition to stabilizing the system, it would also be

possible to reduce the relative building response.

Figures 3a through 3c illustrate the effect of inclination angle of the first-story columns on time-history response of story drift of the building with main period T_1=0.3 sec, under fault-normal pulse with different magnitudes. As it is seen, by increasing of inclination angle of the first-story columns the drift amplitude of the first story decreases, except for inclination angle $\alpha > 10^{\circ}$ and under earthquake magnitude M=7, that the effect of gravity leads to increase the drift amplitude of the first story as well. For upper stories by increasing of inclination angle of the first-story columns the drift amplitude increases.

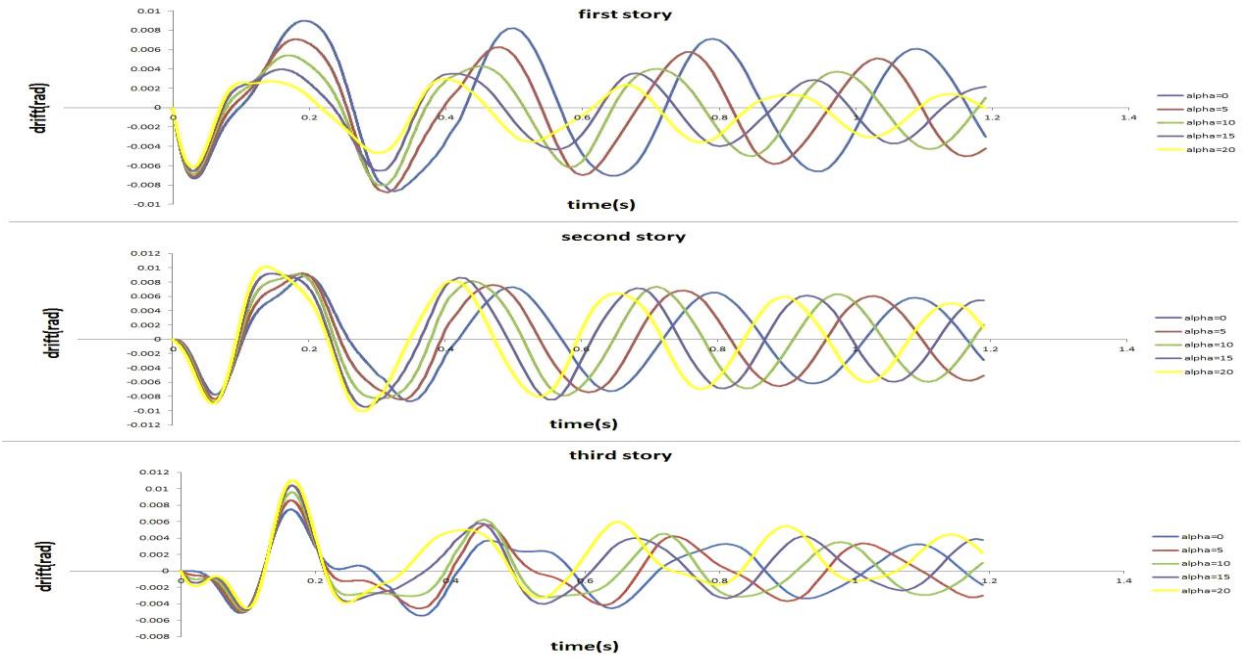

Fig.3a. Effect of inclination angle of the first-story columns on maximum story drift for T_1=0.3 sec, under fault-normal pulse with magnitude M=5

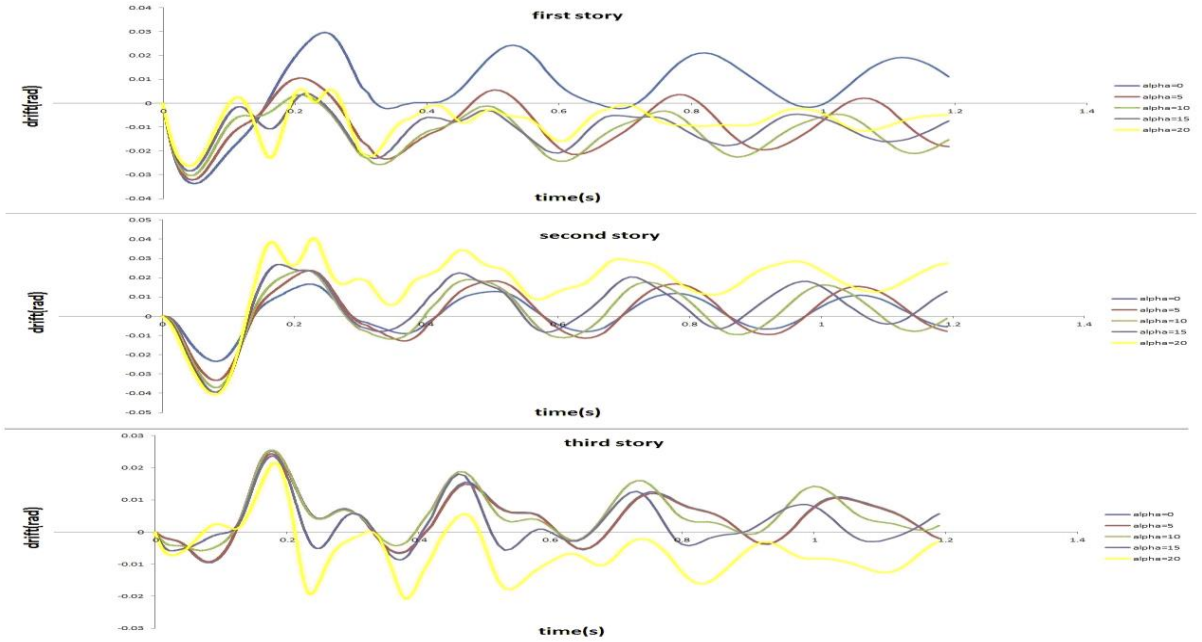

Fig.3b. Same as Fig. 3a except for M =6.

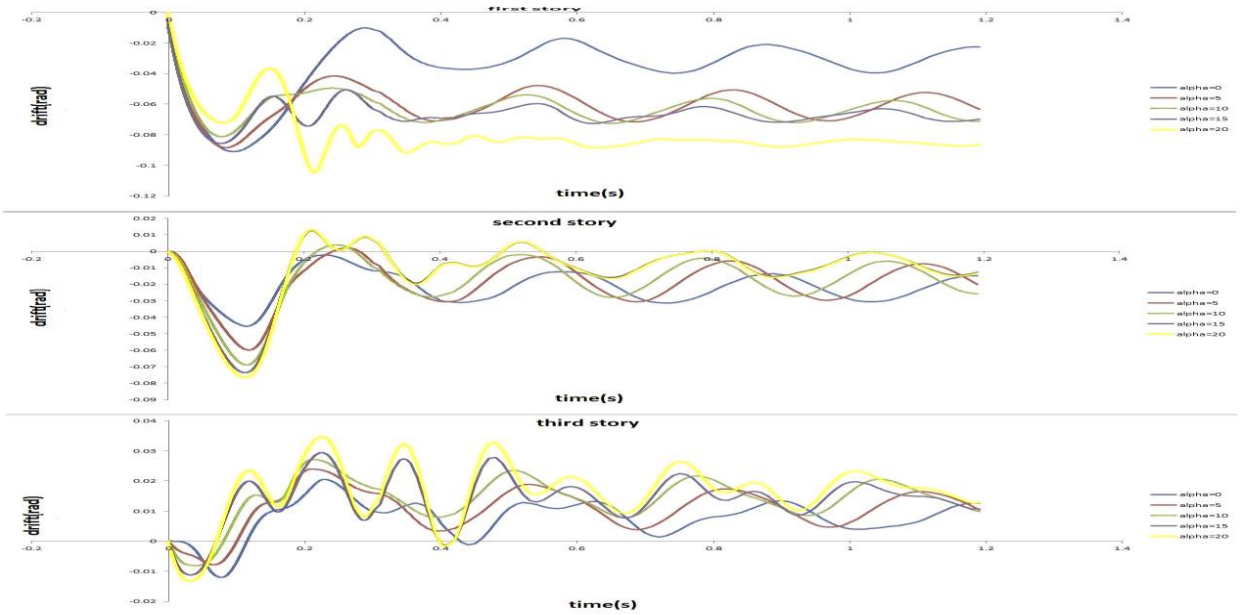

Fig.3c. Same as Fig. 3a except for M =7.

In Figures 4a through 4c the main period of building is T_1=0.6 sec, and the trend is same as Figures 3a through 3c for building with main period T_1=0.3 sec.

In Figure 5b the building with main period T_1=0.3 sec, is subjected to El Centro earthquake (Figure 5a) and the effect of inclination angle of the first-story columns on time-history response of story drift is shown. As it is seen, the inclined first-story columns play important role in decreasing of the first-story drift. Nevertheless, they lead to increase the upper-story drift. This solution would be useful in earthquake resistant design of buildings with architectural limitations at the first story.

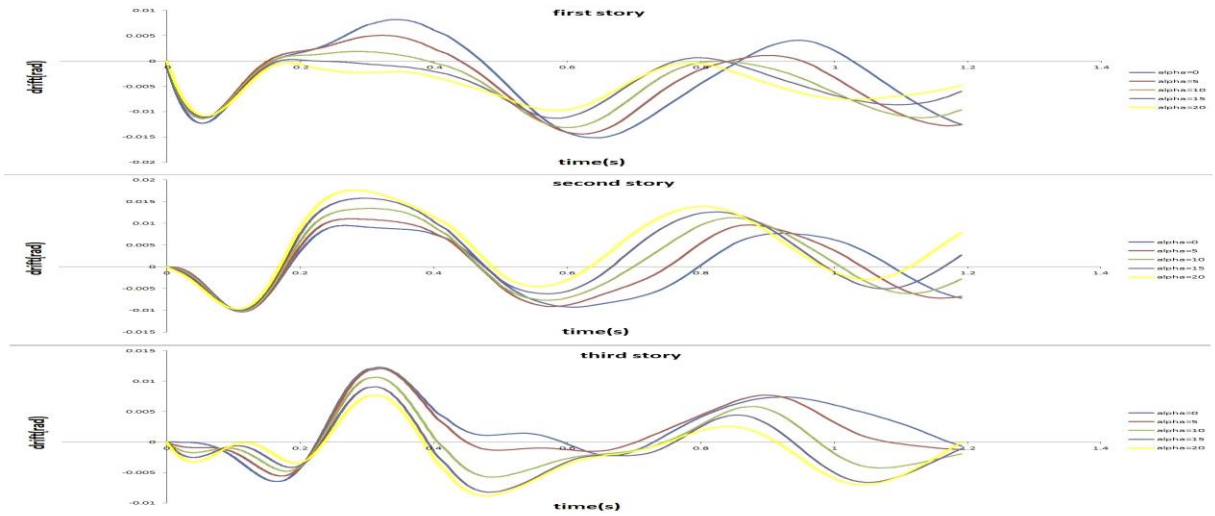

Fig.4a. Effect of inclination angle of the first-story columns on maximum story drift for T_1=0.6 sec, under fault-normal pulse with magnitude M=5

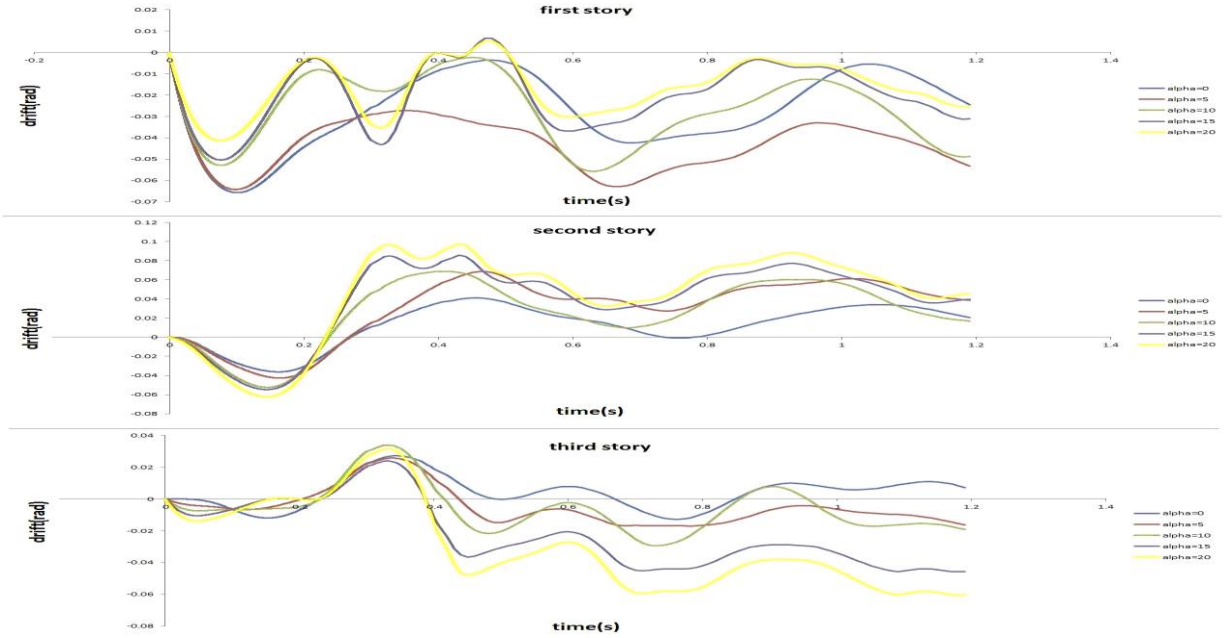

Fig.4b. Same as Fig. 4a except for M =6.

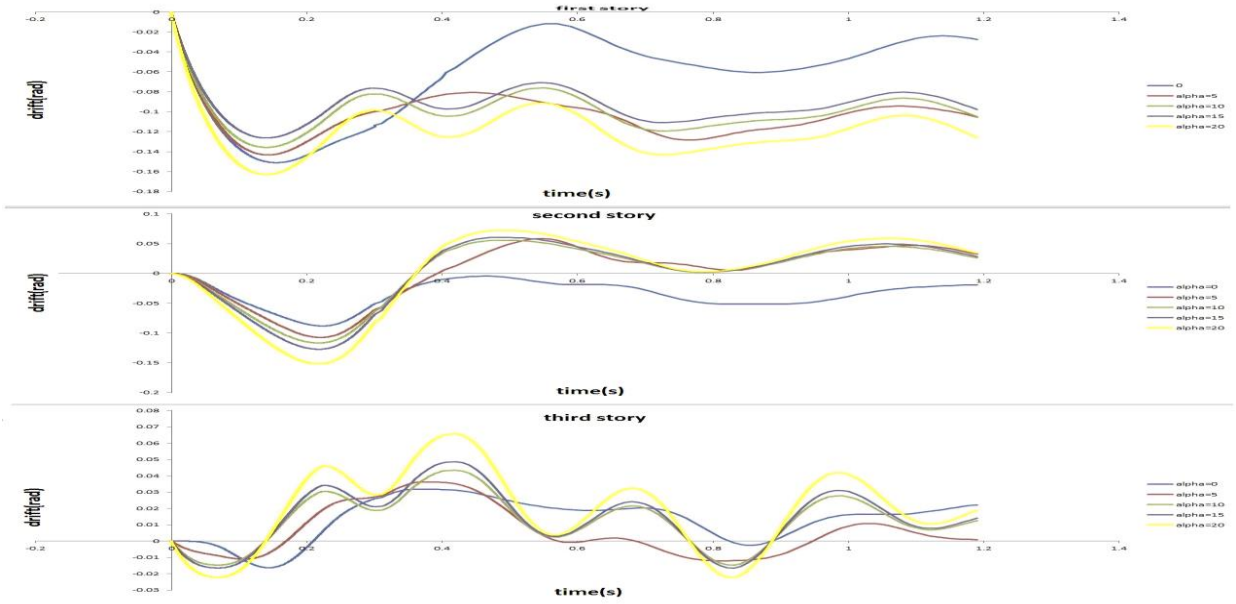

Fig.4c. Same as Fig. 4a except for M =7.

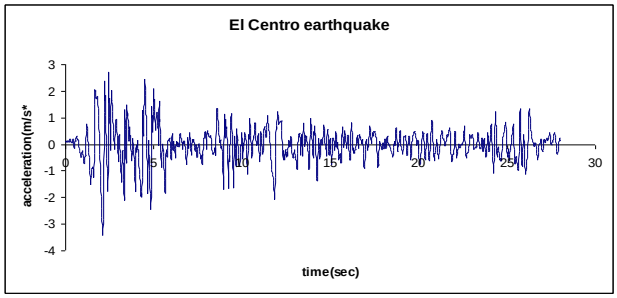

Fig.5a. Acceleration time-history of El Centro earthquake.

Fig.5b

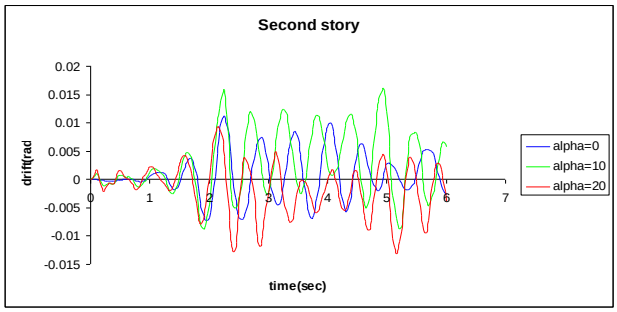

Fig.5b

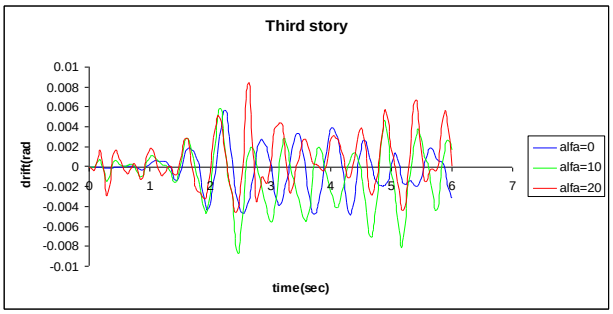

Fig.5b

Fig.5b. Effect of inclination angle of the first-story columns on maximum story drift for T_1=0.3 sec, under El Centro earthquake

REFERENCES

[1] Mavroeidis, G.P., Dong, G., and Papageorgiou, A. S. (2004). "Near-fault ground motions, and the response of elastic and inelastic single-degree-of-freedom (SDOF) systems". *Earthquake Engineering and Structural Dynamics,* 33(9): 1023-1049.

[2] Trifunac, M.D. (1971). "Zero Baseline Correction of Strong-Motion Accelerograms". *Bull. Seism. Soc. Amer.*, 61(5), 1201-1211.

[3] Trifunac, M.D. (1974). "A Three-Dimensional Dislocation Model for the San Fernando, California, Earthquake of February 9, 1971". *Bull. Seism. Soc. Amer.*, 64(1): 149-172.

[4] Bogdanoff, J.L, Goldberg, J.E, and Schiff, A.J. (1965). "The effect of ground transmission time on the response of long structures". *Bull. Seism. Soc. Am.*, 55, 627-640.

[5] Zerva, A. (2009). "Spatial variation of seismic ground motions". CRC Press (Taylor and Francis), London.

[6] Hyun, C. H., Yun, C. B., and Lee, D. G. (1992). " Nonstationary response analysis of suspension bridges for multiple support excitations". *Prob. Eng. Mech.* 7(1), 27-35.

[7] Kashefi, I., and Trifunac, M.D. (1986). "Investigation of earthquake response of simple bridge structures". Dept. of Civil Eng., Report No. CE 86-02, Univ. of Southern California, Los Angeles, CA.

[8] Perotti, F. (1990). "Structural response to non-stationary multiple support random excitation". *Earthquake Eng. Struct. Dyn.*, 19, 513-527.

[9] Todorovska, M. I., and Lee, V. W. (1989). "Seismic waves in buildings with shear walls or central core". *J. Eng. Mech. Div. ASCE*, 115(12), 2669-2686.

[10] Todorovska, M. I., and Trifunac, M.D. (1989). "Antiplane earthquake waves in long structures". *J. eng. mech. div. ASCE,* 115(12), 2687-2708.

[11] Todorovska, M. I., and Trifunac, M.D. (1990a). "A note on the propagation of earthquake waves in buildings with soft first floor". *J. Eng. Mech. Div. ASCE,* 116(4), 892-900.

[12] Todorovska, M. I., and Trifunac, M.D. (1990b). "A note on excitation of long structures by ground waves". *J. Eng. Mech. Div. ASCE,* 116(4), 952-964.

[13] Kojić, S., and Trifunac, M.D. (1988). "Earthquake response of arch dams to nonuniform canyon motion". *Dept. of Civil Eng., Report No. CE 88-03,* Univ. of Southern California, Los Angeles, CA.

[14] Kojić, S., and Trifunac, M.D. (1991a). "Earthquake stresses in arch dams: I-theory and antiplane excitation". *J. Eng. Mech. Div. ASCE,* 117(3), 532-552.

[15] Kojić, S. and Trifunac, M.D. (1991b). "Earthquake stresses in arch dams: II-excitation by SV, P and Rayleigh waves". *J. Eng. Mech. Div. ASCE,* 117(3), 553-574.

[16] Okubo, T., Arakawa, T., and Kawashima, T. (1983). "Preliminary analysis of finite ground strains induced during earthquake and effect of spatial ground motions on structural response". Int. Symp. on Lifeline Earthquake Eng., 4th U.S. National Conf. on Pressure Vessels and Piping Technology, ASME, Portland, Oregon.

[17] Zembaty, Z., and Krenk, S. (1993). "Spatial seismic excitations and reponse spectra". *J. Eng. Mech. Div. ASCE,* 119, 2449-2459.

[18] Zembaty, Z., and Krenk, S. (1994). "Reponse spectra of spatial seismic ground motion". *10th European Conf. Earthquake Eng*. Vol. 2, Vienna, Austria, 1271-1275.

[19] Jalali, R.S., Nouripour Azgomi, M., and Trifunac, M.D (2013). "In-plane response of two-story structures to near-fault ground motion". *Soil Dynamics and Earthquake Engineering*, 55, 263-274.

[20] Todorovska, M. I. (1999). "Base isolation by a soft first story with inclined columns". *J. Eng. Mech. Div. ASCE,* 125(4), 448-457.

[21] Trifunac, M.D., Udwadia, F.E. (1974). "Parkfield, California, earthquake of June 27, 1966: A three-dimensional moving

dislocation". *Bull. Seism. Soc. Amer.*, 64(3): 511-533.

[22] Haskell, N.A. (1969). "Elastic displacements in the near field of a propagating fault". *Bull. Seismol. Soc. Amer.*, 59(2), 956-980.

[23] Trifunac, M.D. (1993a). "Long Period Fourier Amplitude Spectra of Strong Motion Acceleration". *Soil Dynamics and Earthquake Eng*., 12(6), 363-382.

[24] Trifunac, M.D. (1993b). "Broad band extension of Fourier amplitude spectra of strong motion acceleration". *Dept. of Civil Eng. Report CE 93-01*, Univ. of Southern California, Los Angeles, CA.

[25] Trifunac, M.D. (1998). "Stresses and intermediate frequencies of strong motion acceleration". *Geofizika*, 14, 1-27.

[26] Trifunac, M.D., Todorovska, M.I., Lee, V.W. (1998). "The Rinaldi strong motion accelerogram of the Northridge, California, earthquake of 17 January, 1994". *Earthquake Spectra*, 14(1): 225-239.

[27] Trifunac, M. D. (1982). "A note on rotational components of earthquake motions on ground surface for incident body waves". *Soil Dyn. Earthq. Eng.* 1(1), 11-19.

APPENDIX - The dynamic model

Nonlinear equations of motion for three-story building with inclined first-story columns subjected to differential base excitation

As can be seen from Fig. 1, the model we consider is a three-story building with inclined first-story columns consisting of three rigid beams with mass mi, polar moment inertia Ii, and length L supported by rigid massless columns connected at two ends by circular springs. The stiffness of the springs is assumed to be bilinear, as shown in Fig. A1.a. The massless columns are connected at two ends by circular dashpots providing the fraction of critical damping. Rotation of the columns is assumed not to be small, which leads us to consider the geometric nonlinearity. The masses are acted upon by the acceleration of gravity, g, and are excited by differential ground motions at two piers. The deformed shape and all forces that act on the structural model, including the D'Alembert's forces and moments, are shown in Figs.A2, and A3, respectively. We define the parameters of the model as follows:

k_{ϕ_i} = Initial rotational stiffness of column springs of i-th story

c_{ϕ_i} = Linear rotational damping coefficient of columns of i-th story

m_i = Mass of rigid beam of i-th story

L= Length of rigid beam

$I_i = \frac{1}{12} m_i L^2$ = Polar moment inertia of rigid beam of i-th story

h_i = Height of i-th story

ψ_{1i} = Relative rocking angle of $i-th$ column of the first story

$\phi_{11} = \theta_{g_1} + \psi_{11} + \delta_1$ = Absolute rocking angle of the first column of the first story

$\phi_{12} = \theta_{g_2} + \psi_{12} + \delta_2$ = Absolute rocking angle of the second column of the first story

ϕ_{ji} = Relative rocking angle of $i-th$ column of $j-th$ story (i=1, 2; j=2, 3)

$u_{g_i}, v_{g_i}, \theta_{g_i}$ = The free-field horizontal, vertical, and rotational motions of ground surface at the base of $i-th$ column $(i = 1, 2)$

$U_{G_i}, V_{G_i}, \theta_{G_i}$ = Absolute horizontal, vertical, and rotational motions of the center of gravity of *i-th* rigid beam.

$\delta_1 = -\delta_2 = \alpha =$ The inclination angle of the first-story columns respect to the vertical axes

According to Fig.A2, and because of the rigidity of the columns and beams, we can write the following relations between the displacements of beams and columns.

Absolute horizontal and vertical displacements of i-th beam ends:

Absolute horizontal and vertical displacements of the top of the first-story columns:

$$
\begin{aligned}
&u_{T_{i1}} = U_{G_i} + \frac{L}{2}(1-\cos\theta_{G_i}) \\
&u_{T_{i2}} = U_{G_i} - \frac{L}{2}(1-\cos\theta_{G_i}) \\
&v_{T_{i1}} = V_{G_i} + \frac{L}{2}\sin\theta_{G_i} \\
&v_{T_{i2}} = V_{G_i} - \frac{L}{2}\sin\theta_{G_i} \\
&i = 1,2,3
\end{aligned}
\tag{A.1}
$$

$$
\begin{aligned}
&u_{T_{11}} = u_{g_1} + \frac{h_1}{\cos\alpha}(\sin\phi_{11} - \sin\delta_1) \\
&u_{T_{12}} = u_{g_2} + \frac{h_1}{\cos\alpha}(\sin\phi_{12} - \sin\delta_2) \\
&v_{T_{11}} = v_{g_1} + \frac{h_1}{\cos\alpha}(\cos\phi_{11} - \cos\delta_1) \\
&v_{T_{12}} = v_{g_2} + \frac{h_1}{\cos\alpha}(\cos\phi_{12} - \cos\delta_2)
\end{aligned}
\tag{A.2}
$$

Absolute horizontal and vertical displacements of the top of i-th story columns:

$$
\begin{aligned}
&u_{T_{i1}} = u_{T_{(i-1)1}} + h_i \sin(\theta_{G_{i-1}} + \phi_{i1}) \\
&v_{T_{i1}} = v_{T_{(i-1)1}} - h_i\left[1-\cos\left(\theta_{G_{i-1}} + \phi_{i1}\right)\right] \\
&u_{T_{i2}} = u_{T_{(i-1)2}} + h_i \sin(\theta_{G_{i-1}} + \phi_{i2}) \\
&v_{T_{i2}} = v_{T_{(i-1)2}} - h_i\left[1-\cos\left(\theta_{G_{i-1}} + \phi_{i2}\right)\right] \\
&i = 2,3
\end{aligned}
\tag{A.3}
$$

By combining equations (A.1), (A.2), and (A.3), we find the absolute motions of the rigid beams as follows:

$$
\begin{aligned}
&U_{G_1} = \frac{1}{2}\left[u_{g_1} + u_{g_2} + \frac{h_1}{\cos\alpha}\left(\sin\phi_{11} + \sin\phi_{12}\right)\right] \\
&V_{G_1} = \frac{1}{2}\left[v_{g_1} + v_{g_2} + \frac{h_1}{\cos\alpha}\left(\cos\phi_{11} + \cos\phi_{12} - \cos\delta_1 - \cos\delta_2\right)\right] \\
&\theta_{G_1} = sin^{-1}\left[\frac{1}{L}\left(v_{g_1} - v_{g_2} + \frac{h_1}{\cos\alpha}\left(\cos\phi_{11} - \cos\phi_{12}\right)\right)\right]
\end{aligned}
$$

$$
\begin{aligned}
&U_{G_i} = U_{G_{i-1}} + \frac{h_i}{2}\left[\sin(\theta_{G_{i-1}} + \phi_{i1}) + \sin(\theta_{G_{i-1}} + \phi_{i2})\right] \\
&V_{G_i} = V_{G_{i-1}} - \frac{h_i}{2}\left[2 - \cos(\theta_{G_{i-1}} + \phi_{i1}) - \cos(\theta_{G_{i-1}} + \phi_{i2})\right] \\
&\theta_{G_i} = sin^{-1}\left\{\sin\theta_{G_{i-1}} + \frac{h_i}{L}\left[\cos(\theta_{G_{i-1}} + \phi_{i1}) - \cos(\theta_{G_{i-1}} + \phi_{i2})\right]\right\} \\
&i = 2,3
\end{aligned}
\tag{A.4}
$$

According to Fig.A3 we can obtain the system of equations of motion of the model as follows

$$
\begin{cases}
c_{11}\ddot{\phi}_{11} + c_{12}\ddot{\phi}_{12} + c_{13}\ddot{\phi}_{21} + c_{14}\ddot{\phi}_{22} + c_{15}\ddot{\phi}_{31} + c_{16}\ddot{\phi}_{32} + c_{17} = 0 \\
c_{21}\ddot{\phi}_{11} + c_{22}\ddot{\phi}_{12} + c_{23}\ddot{\phi}_{21} + c_{24}\ddot{\phi}_{22} + c_{25}\ddot{\phi}_{31} + c_{26}\ddot{\phi}_{32} + c_{27} = 0 \\
c_{31}\ddot{\phi}_{11} + c_{32}\ddot{\phi}_{12} + c_{33}\ddot{\phi}_{21} + c_{34}\ddot{\phi}_{22} + c_{35}\ddot{\phi}_{31} + c_{36}\ddot{\phi}_{32} + c_{37} = 0
\end{cases}
\tag{A.5}
$$

Where c_{ij} are nonlinear functions of $\phi_{ij}, \dot{\phi}_{ij}, \alpha$, and base excitations. Because of differential ground motion, the system has six degrees of freedom—three independent and three dependent. For the solution of Eq. (A.5), we need three other equations that represent geometric relations in the model. Because of the assumed rigidity of beams, their lengths are constant. Therefore, for the deformed shape of the model we can write the following relations for three beams:

$$\begin{aligned}
&(L+u_{T_{12}}-u_{T_{11}})^2+(v_{T_{12}}-v_{T_{11}})^2=L^2\\
&(L+u_{T_{22}}-u_{T_{21}})^2+(v_{T_{22}}-v_{T_{21}})^2=L^2\\
&(L+u_{T_{32}}-u_{T_{31}})^2+(v_{T_{32}}-v_{T_{31}})^2=L^2
\end{aligned} \tag{A.6}$$

Taking the first and second derivatives of Eq. (A.6) with respect to time and substituting into Eq. (A.5) gives

$$\begin{cases}
z_{11}\ddot{\psi}_{11}+z_{12}\ddot{\phi}_{21}+z_{13}\ddot{\phi}_{31}+z_{14}=0\\
z_{21}\ddot{\psi}_{11}+z_{22}\ddot{\phi}_{21}+z_{23}\ddot{\phi}_{31}+z_{24}=0\\
z_{31}\ddot{\psi}_{11}+z_{32}\ddot{\phi}_{21}+z_{33}\ddot{\phi}_{31}+z_{34}=0
\end{cases} \tag{A.7}$$

Where z_{ij} are nonlinear functions of $\psi_{11}, \phi_{21}, \phi_{31}, \dot{\psi}_{11}, \dot{\phi}_{21}, \dot{\phi}_{31}, \alpha$, and input ground motion.

Equation (A.7) is a system of coupled, nonlinear differential equations for $\psi_{11}, \phi_{21},$ and ϕ_{31} that can be solved by numerical methods. Floor masses and story stiffness vary linearly from top to bottom as follows. Their relative values are so proportioned that the fundamental period of vibration of the building is nearly equal to *0.1N*, *N* being the number of stories in the building.

$$\begin{aligned}
&m_j=(1.0-0.4\frac{j-1}{N-1})m_1\\
&k_{\phi_j}=(1.0-0.4\frac{j-1}{N-1})k_{\phi_1}\\
&j=1,2,...,N
\end{aligned} \tag{A.8}$$

We suppose that the floor damping coefficients vary linearly from top to bottom as well:

$$\begin{aligned}
&c_{\phi_j}=(1.0-0.4\frac{j-1}{N-1})c_{\phi_1}\\
&j=1,2,...,N
\end{aligned} \tag{A.9}$$

For small deformations of a linear system, and by neglecting gravity, damping, input ground motion, and high-order parameters, and by taking the Fourier transform of Eq. (A.7) we would have

$$\left[K-\omega^2 M\right]\begin{Bmatrix}\psi_{11}\\ \phi_{21}\\ \phi_{31}\end{Bmatrix}=\begin{Bmatrix}0\\0\\0\end{Bmatrix},$$

$$[K]=\begin{bmatrix} \left(\frac{8K_{\phi_1}\tan\alpha\sin\alpha}{L^2}+\frac{4K_{\phi_1}\sin\alpha}{Lh_1}+\frac{4K_{\phi_1}\tan\alpha}{Lh_1}+\frac{4K_{\phi_1}}{h_1^2}+\frac{4K_{\phi_2}}{h_2^2}-\frac{8K_{\phi_2}\tan\alpha}{Lh_2}\right) & \left(-\frac{4K_{\phi_2}}{h_2^2}+\frac{8K_{\phi_2}\tan\alpha}{Lh_2}-\frac{8K_{\phi_3}\tan\alpha}{Lh_3}\right) & \frac{8K_{\phi_3}\tan\alpha}{Lh_3} \\ -\frac{4K_{\phi_2}}{h_2^2} & \left(\frac{4K_{\phi_2}}{h_2^2}+\frac{4K_{\phi_3}}{h_3^2}\right) & -\frac{4K_{\phi_3}}{h_3^2} \\ 0 & -\frac{4K_{\phi_3}}{h_3^2} & \frac{4K_{\phi_3}}{h_3^2} \end{bmatrix}$$

$$[\mathbf{M}]=\begin{bmatrix} \left(m_1\cos\alpha+\frac{0.344h_1^2\tan\alpha\sin\alpha}{L^2}(m_1+m_2+m_3)\right) & 0 & 0 \\ \left(m_2(\cos\alpha-\frac{2h_2\sin\alpha}{L})-m_2\right) & m_2 & 0 \\ \left(m_3(\cos\alpha-\frac{4h_3\sin\alpha}{L})-m_3\right) & 0 & m_3 \end{bmatrix}$$

(A.10)

As it is seen from the above equation the stiffness and the mass matrices are not symmetric. For $\alpha=0$ the stiffness and the mass matrices are same as those for common shear building. For nonzero solution of Eq. (A.10), the determinant of the coefficients should be zero. Therefore, the characteristic equation of the model would be

$$\left|K-\omega^2M\right|=0$$

(A.11)

By solving Eq. (A.11), one can find the rotational stiffness of columns and natural frequencies of the model. For example for $\alpha=10^\circ$ we have

$$\begin{cases} T_1=0.3 \\ \alpha=0 \end{cases} \xrightarrow{Eq.(A.11)} \frac{k_{\phi_1}}{m_1h_1^2}=449 \xrightarrow[\alpha=10^\circ]{Eq.(A.11)} \begin{cases} \omega_1=22.11 \\ \omega_2=49.77 \\ \omega_3=72.03 \end{cases}$$

For $\alpha=0$, we can determine the rotational damping coefficient of columns for a prescribed fraction of critical damping. The mass, stiffness, and damping matrices of the model are

$$[M]=\begin{bmatrix} m_1 & 0 & 0 \\ 0 & m_2 & 0 \\ 0 & 0 & m_3 \end{bmatrix},$$

$$[K]=\begin{bmatrix} \left(\frac{4k_{\phi_1}}{h_1^2}+\frac{4k_{\phi_2}}{h_2^2}\right) & -\frac{4k_{\phi_2}}{h_2^2} & 0 \\ -\frac{4k_{\phi_2}}{h_2^2} & \left(\frac{4k_{\phi_2}}{h_2^2}+\frac{4k_{\phi_3}}{h_3^2}\right) & -\frac{4k_{\phi_3}}{h_3^2} \\ 0 & -\frac{4k_{\phi_3}}{h_3^2} & \frac{4k_{\phi_3}}{h_3^2} \end{bmatrix},$$

$$[C]=\begin{bmatrix} \left(\frac{4c_{\phi_1}}{h_1^2}+\frac{4c_{\phi_2}}{h_2^2}\right) & -\frac{4c_{\phi_2}}{h_2^2} & 0 \\ -\frac{4c_{\phi_2}}{h_2^2} & \left(\frac{4c_{\phi_2}}{h_2^2}+\frac{4c_{\phi_3}}{h_3^2}\right) & -\frac{4c_{\phi_3}}{h_3^2} \\ 0 & -\frac{4c_{\phi_3}}{h_3^2} & \frac{4c_{\phi_3}}{h_3^2} \end{bmatrix}$$

In modal space we would have

$$[M_n]=[\Phi]^T[M][\Phi]=\begin{bmatrix} M_1 & 0 & 0 \\ 0 & M_2 & 0 \\ 0 & 0 & M_3 \end{bmatrix},$$

$$[K_n]=[\Phi]^T[K][\Phi]=\begin{bmatrix} K_1 & 0 & 0 \\ 0 & K_2 & 0 \\ 0 & 0 & K_3 \end{bmatrix},$$

$$[C_n]=[\Phi]^T[C][\Phi]=\begin{bmatrix} C_1 & 0 & 0 \\ 0 & C_2 & 0 \\ 0 & 0 & C_3 \end{bmatrix}$$

The damping ratio of *i-th* mode would be

$$\xi_i=\frac{C_i}{2M_i\omega_i}\ .$$

So, by assuming that the damping ratio of the first mode is equal to $\xi_1=0.02$, one would have the rotational damping coefficient of columns as follows:

$$\xi_1=0.02\Rightarrow\frac{c_{\phi_1}}{m_1h_1^{\ 2}}=0.86$$

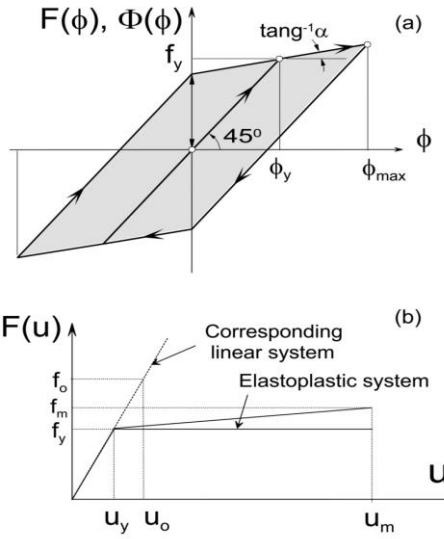

Fig. A1. (a) Bilinear rotational stiffness models, (b) elasto-plastic system and the corresponding linear system.

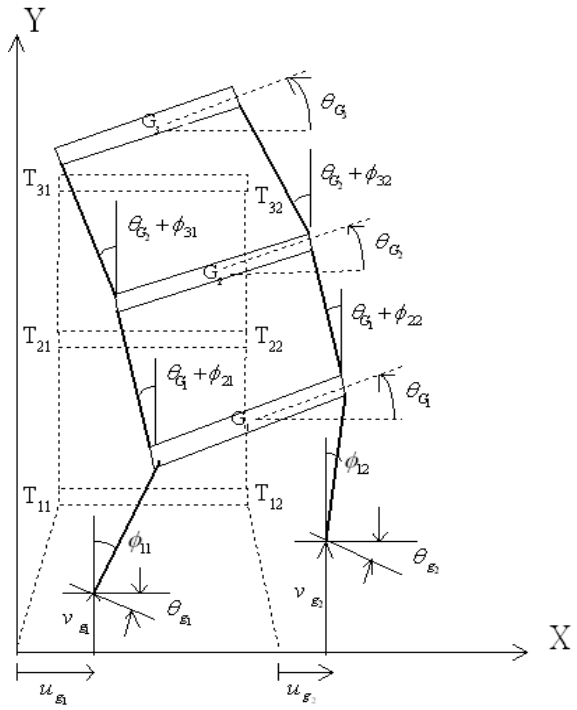

Fig. A2. Deformed shape of the model in Fig. 1, subjected to differential motions at the base of its columns.

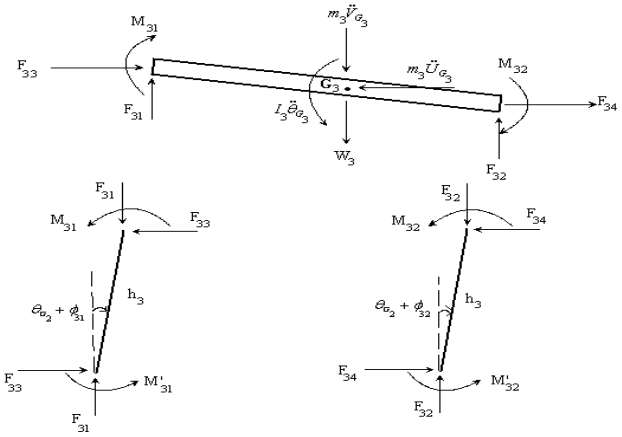

(a)

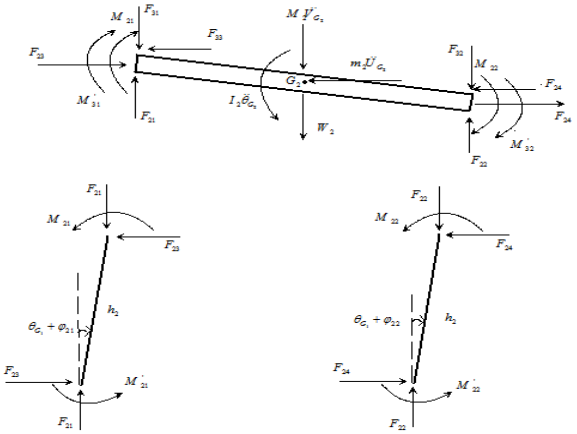

(b)

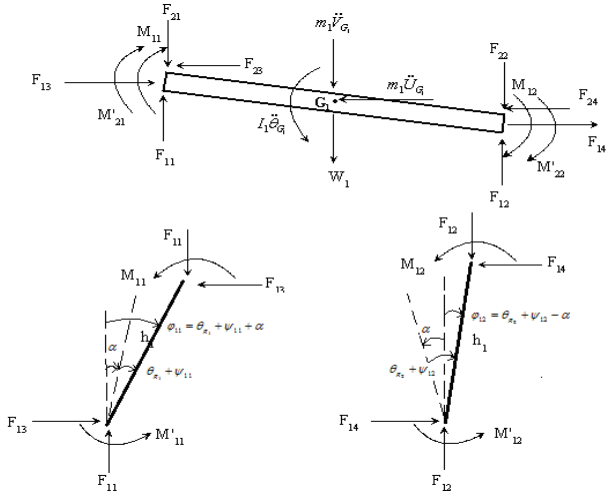

(c)

Fig. A3, (a) Free-body diagrams for the third story, (b) the second story, and (c) the first story of the model in Fig. 1.